Thin Solid Films 551 (2014) 131–135

Contents lists available at ScienceDirect

Thin Solid Films

journal homepage: www.elsevier.com/locate/tsf

Dependence of the performance of inverted polymer solar cells on thickness of an electron selective ZnO layer deposited by magnetron sputtering

Feng Zhu [a], Xiaohong Chen [a,*], Lin Zhou [a], Jianping Zhou [b], Jiaxiang Yang [c], Sumei Huang [a], Zhuo Sun [a]

[a] Engineering Research Center for Nanophotonics and Advanced Instrument, Ministry of Education and Department of Physics, East China Normal University, Shanghai 200062, China
[b] School of Power and Automation Engineering, Shanghai University of Electric Power, Shanghai 2000902, China
[c] Department of Chemistry, Anhui University, Hefei, Anhui Province 230039, China

ARTICLE INFO

Article history:
Received 24 May 2013
Received in revised form 21 November 2013
Accepted 22 November 2013
Available online 1 December 2013

Keywords:
Polymer solar cells
Magnetron sputtering
Zinc oxide
Negative capacitance

ABSTRACT

The performance of inverted polymer solar cells (PSCs) was investigated using ZnO layer as an electron selective layer ranging from 15 nm to 60 nm thickness by magnetron sputtering deposition. The average power conversion efficiency (PCE) of inverted poly(3-hexylthiophene) and phenyl-C_{61}-butyric acid methylester (P3HT:PCBM) based PSCs with 15 nm and 30 nm thickness ZnO layer respectively reaches 3.63% and 3.45%, which is comparable to that of traditional PSCs with poly(3,4-ethylenedioxythiophene)/poly(styrenesulfonate) anode buffer layer. The deteriorated PCE 2.65% of PSCs with 60 nm ZnO layer is attributed to the intensive surface roughness of ZnO layer by atomic force microscopy images. The increasing PCE 3.44% of PSCs with ionic liquid-functionalized carbon nanoparticles (ILCNs) modified 60 nm ZnO layer suggested that the interface contact at the interface of ZnO/P3HT:PCBM was significantly improved by ILCNs modification. The always positive capacitive behavior of PSCs with 15 nm, 30 nm and ILCNs modified 60 nm ZnO layer further demonstrated their superior interface contact at ZnO/P3HT:PCBM compared to PSCs with 60 nm ZnO layer due to its negative capacitance.

1. Introduction

Polymer solar cells (PSCs) have attracted considerable attention due to their unique properties such as mechanical flexibility, light weight and low cost. The main challenges are improving power conversion efficiency (PCE) and lifetime of PSCs [1,2]. The PCE of PSCs has been quickly increased from 3–4% based on poly(3-hexylthiophene) and phenyl-C_{61}-butyric acid methylester (P3HT:PCBM) blended film to 9–10% using low band-gap polymer blended with phenyl-C_{70}-butyric acid methylester in the past several years [3,4]. In conventional PSCs, poly(3,4-ethylenedioxythiophene)/poly(styrenesulfonate) (PEDOT:PSS) as a hole conducting layer is spin-coated on top of tin-doped indium oxide (ITO) substrate to aid hole extraction. The active layer is sandwiched between an ITO/PEDOT:PSS anode and a low work function metal cathode, such as Al or Ca/Ag. However, PEDOT:PSS is detrimental to ITO anode due to its acidic property, leading to reducing device lifetime [5,6]. The n-type and p-type transparent metal oxides have been recently selected for cathode and anode contacts in PSCs, providing flexibility of designing device structures including inverted PSCs [1,7,8]. The inverted PSCs can effectively solve some disadvantages of traditional PSCs with PEDOT:PSS anode contact layer by using n-type and p-type metal oxides as cathode and anode contacts, respectively.

An n-type metal oxide ZnO has been extensively demonstrated as a good electron collection material due to its high electron mobility and high transparency in the visible wavelength range. The ZnO layer deposited by a sol–gel process was adopted by Kyaw et al. in inverted P3HT:PCBM based PSCs and achieved a PCE of 3.09% [8]. Hau et al. reported that PCE of inverted P3HT:PCBM based PSCs can reach 3.78% and 3.58% through spin-coating ZnO nanoparticles on the glass and plastic substrates, respectively [9]. However, the solution-processed ZnO layer need be annealed under high temperature to increase the carrier mobility, limiting its application in plastic substrates. The performance of PSCs based on ZnO nanoparticles layer strongly depends on the control of particle size and layer thickness is difficult. Recently, Wang et al. reported highly efficient inverted PSCs using atomic layer deposition grown ZnO as an electron selective layer. Atom layer deposition is a kind of chemical vapour deposition technique, easily controlling film thickness and achieving superior film quality at low temperature [10]. Magnetron sputtering method is also an excellent and mature depositing film technology due to its unique advantages, such as easily precisely controlling film composition and thickness, strong operability and batch production. Moreover, directional deposition film can avoid the pollution of the substrate back during roll-to-roll coating processes [11]. Some groups reported the relatively low PCE of PSCs with ZnO

* Corresponding author. Tel.: +86 21 62233676.
E-mail address: xhchen@phy.ecnu.edu.cn (X. Chen).

0040-6090/$ – see front matter.
http://dx.doi.org/10.1016/j.tsf.2013.11.096

deposited on P3HT:PCBM layer or inverted PSCs with ZnO deposited on the ITO surface using magnetron sputtering method [12,13]. Considering present commercial ITO electrode, as well as more and more universal emerging electrodes, such as aluminum-doped zinc oxide and metal oxide/metal/metal oxide [14–16], fabricated with magnetron sputtering technology, developing ZnO and other transparent metal oxides as a buffer layer deposited with the same method in PSCs are becoming more and more urgent and practical. The compatible procedure of electrode and buffer layer is helpful to simplify procedure and control cost of PSCs. In addition, magnetron sputtering method is also a kind of encapsulation technology for organic solar cells and PSCs with depositing AlO_x, SiO_x, $Al_2O_3/Ag/Al_2O_3$ layer against in-diffused moisture and oxygen [17]. This method is easily compatible with other vacuum encapsulation process such as ALD [18], and other chemical vapour deposition process [19]. In this paper, P3HT:PCBM blends, as previous typical photoactive layer, was still chosen to act as photoactive layer in inverted PSCs, different thick ZnO film was deposited as an electron selective layer by magnetron sputtering technique without adding substrate temperature. The average PCE of inverted PSCs based on P3HT:PCBM blend was apparently decreased from 3.63% to 2.65% with increasing ZnO thickness from 15 nm to 60 nm.

2. Experiments

The ZnO layer was deposited onto ITO coated glass substrate by magnetron sputtering with RF power 50 W and working pressure 0.3 Pa under a base pressure of 3.0×10^{-3} Pa, using a commercial ZnO target of 99.99% purity. A total gas flow of 20 sccm with 1:7 of O_2/Ar ratio was kept in all sputtering samples. The ionic liquid-functionalized carbon nanoparticles (ILCNs) were synthesized by the electrochemical exfoliation of graphite electrode in 1-butyl-3-methylimidazolium tetrafluoroborate ([C4min] + [BF4]−) and water mixture (40:60). The below 4 nm size of ILCNs was observed by transmission electron microscopy images [20]. The details of ILCNs synthesis and its properties have been reported [20,21]. The ILCNs were spin-coated on top of ZnO film to modify ZnO film surface. Solutions containing P3HT and PCBM with 1:0.8 wt. ratio were dissolved in 1, 2-dichlorobenzene with 20 mg/ml of P3HT concentration. The 200 nm thickness P3HT:PCBM film was spin-coated on top of the ZnO surface at 800 rpm for 60 s, and then kept in a petri dish for slow growth. After at least 5 h, P3HT:PCBM films were annealed at 120 °C for 10 min. Finally, the 14 nm thickness MoO_3 and 150 nm Al electrode were thermally evaporated onto P3HT:PCBM blend to form an anode under a background pressure of 4.0×10^{-4} Pa. The active area of PSCs is 0.1 cm^{-2}. Current–voltage characteristics were measured under AM1.5G illumination intensity of 100 mW/cm^2 using a Newport solar simulator system. The surface morphologies of ZnO films were measured using atomic force microscopy (AFM, NanoWizard II) and scanning electron microscopy (SEM, FEI; Quanta 200 FEG).

3. Results and discussion

Fig. 1 shows the optical transmittance spectra of different thickness ZnO film on ITO coated glass substrate. The average optical transmittance of ZnO/ITO coated glass ranging from 400 nm to 700 nm doesn't significantly decrease compared with that of pure ITO coated glass. Its transmittance curve trend of red-shift and relative lower transmittance in the short wavelength compared with pure ITO is similar to that of ZnO films coated with solution method [22]. The overall transparency of ILCNs-modified ZnO surface also doesn't affect its transparency, as previous report of ILCNs modified ITO glass [23]. This means that the optical absorption of PSCs made from ZnO/ITO coated glass is almost the same as that of PSCs with ILCNs modified ZnO/ITO coated glass. Therefore, the various PCE of PSCs based on ZnO/ITO electrode isn't attributed to their optical absorption difference.

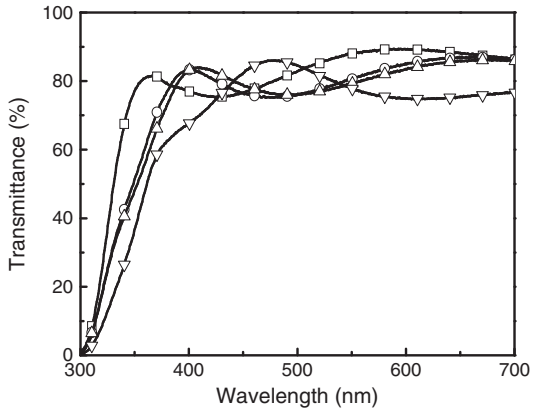

Fig. 1. Optical transmittance spectra of different thickness ZnO film on ITO coated glass substrate. Reference ITO (□), and depositing ZnO film with thickness 15 nm (○), 30 nm (△) and 60 nm (▽) onto the ITO surface.

To investigate the effect of ZnO buffer layer on PCE of inverted PSCs based on P3HT:PCBM blend, we fabricated sets of six types of devices. The current density–voltage (*J–V*) curves of devices with different thickness ZnO buffer layer are shown in Fig. 2 (a). The PCE of PSCs gradually decreased with ZnO buffer layer thickness increasing from 15 nm to 60 nm. After ILCNs modified ZnO film, PCE of PSCs significantly increases for 60 nm thickness ZnO buffer layer, as illustrated in Fig. 2 (b). Table 1 shows average and scatter parameters for traditional and inverted PSC structures. The open voltage (V_{oc}), fill factor (FF) and PCE of PSCs with

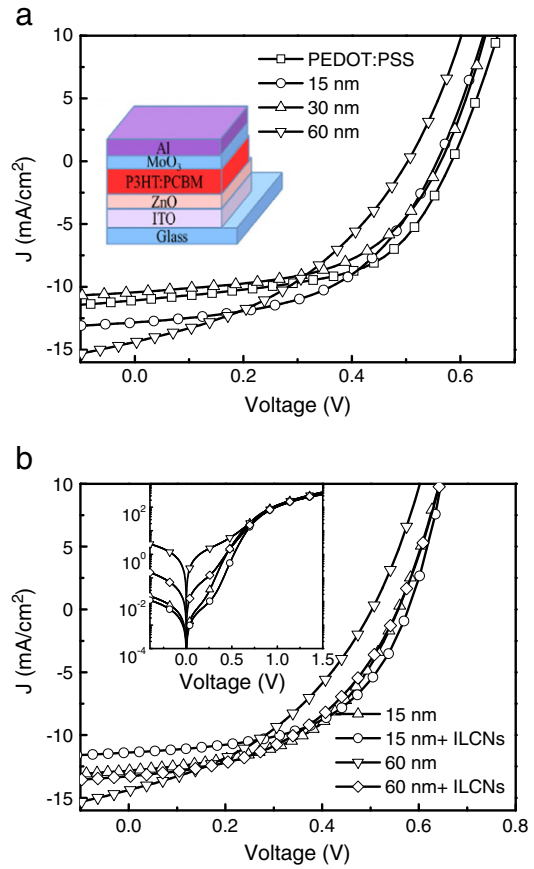

Fig. 2. The *J–V* characteristics of different types of representative PSCs. (a) traditional PSC (□), and inverted PSCs with ZnO layer thickness of 15 nm (○), 30 nm (△), 60 nm (▽); (b) inverted PSCs based on 15 nm thickness ZnO layer modified without (△)/with (○) ILCNs, and 60 nm thickness ZnO layer modified without (▽)/with (◇) ILCNs. The inset of (a) is the structure of inverted PSC; the inset of (b) is dark *J–V* curves.

Table 1
Average and scatter parameters of traditional PSCs and inverted PSCs based on ZnO layers modified with/without ILCNs. Data in parentheses presents the scatter value of PSCs. R_s and R_{sh} are derived from J–V curves at V_{oc} and 0 V, respectively.

Device type [ITO/(buffer layer)]	V_{OC} (V)	J_{SC} (mAcm^{-2})	FF	PCE (%)	R_s (Ω/cm^2)	R_{sh} (Ω/cm^2)
PEDOT	0.57 (±0.01)	11.1 (±1.2)	0.55 (±0.02)	3.57 (±0.5)	10.1	266
ZnO (15 nm)	0.56 (±0.01)	12.4 (±0.7)	0.51 (±0.05)	3.63 (±0.4)	10.6	279
ZnO (30 nm)	0.55 (±0.01)	11.2 (±0.2)	0.50 (±0.02)	3.45 (±0.2)	10.7	337
ZnO (60 nm)	0.50 (±0.02)	14.3 (±1.2)	0.40 (±0.03)	2.65 (±0.2)	13.2	103
ZnO (15 nm)/ILCNs	0.57 (±0.02)	11.4 (±0.5)	0.54 (±0.02)	3.52 (±0.2)	10.7	431
ZnO (60 nm)/ILCNs	0.56 (±0.02)	13.2 (±0.4)	0.47 (±0.02)	3.44 (±0.3)	11.4	308

ILCNs-modified 60 nm thick ZnO buffer layer are obviously larger than that of PSCs with only 60 nm ZnO layer. The average PCE of PSCs with ILCNs-modified 60 nm ZnO layer is almost close to that of PSCs with 15 nm ZnO layer or traditional PSCs. However, the performance of PSCs with 15 nm ZnO layer have no clearly effect after modified with ILCNs. The PCE of PSCs with 15 nm ZnO layer modified with/without ILCNs is almost comparable to that of traditional PSCs with PEDOT:PSS buffer layer. The improving PCE of PSCs with ILCNs-modified 60 nm ZnO layer is attributed to reducing the contact resistance [24] and obviously reverse saturation current, as shown in the inset of Fig. 2 (b). The increasing leakage current and low shunt resistance of PSCs with 60 nm ZnO layer results in deteriorated FF (~0.4) and V_{oc} (0.5 V). Its series resistance (R_s) was decreased from 13.2 Ω/cm^2 to 11.4 Ω/cm^2 after modified with ILCNs, suggesting that the deteriorated FF and Voc are not primarily ascribed to the bulk resistance of ZnO layer. The similar serial resistance of PSCs with 15 nm ZnO layer modified with/without ILCNs indicates that interface contact barrier of ZnO/P3HT:PCBM cannot be further improved after modified ILCNs. This suggests that interface properties of ZnO layer can be varied with increasing ZnO layer thickness, resulting in different PCE of PSCs.

To analyze surface properties of ZnO layer, surface morphologies of different thickness ZnO films were investigated by AFM and SEM, respectively. The surface morphologies of ZnO films on ITO coated glass substrates are shown in Fig. 3. The surface roughness and height difference become larger with increasing thickness of ZnO film. The root mean square surface roughness of 15 nm, 30 nm, 60 nm thickness ZnO layer and ILCNs-modified 60 nm ZnO layer are 1.94 nm, 2.13 nm, 3.12 nm and 1.78 nm, respectively. This indicates that surface roughness of ZnO layer was gradually increased with increasing ZnO layer thickness. However, the intensive surface roughness of 60 nm ZnO layer was inhibited after modified with ILCNs. The morphology variance of ZnO films from SEM images cannot be clearly distinguished due to the low resolution. However, we still can draw a conclusion that the surface roughness of 60 nm ZnO film is greatly increased compared with 15 nm and 30 nm ZnO layer. The increasing roughness of ZnO layer can easily form the pinholes in the active layer [25]. The significantly reverse saturation current and low shunt resistances (R_{sh}) of PSCs with 60 nm ZnO layer are consistent with this speculation, resulting in low FF and V_{oc}. However, the increasing roughness of ZnO layer can increase light scattering and improve light absorption of PSCs [26,27]. The obviously increasing short photocurrent (J_{sc}) of PSCs with 60 nm ZnO layer compared to PSCs with 15 nm and 30 nm ZnO layer is possibly attributed to improving light absorption.

ILCNs as a good interfacial modification material have been demonstrated greatly decreasing work function of ITO after modified with ILCNs [23]. The serial resistance of PSCs with 60 nm ZnO layer was decreased from 13.2 Ω/cm^2 to 11.4 Ω/cm^2 and its R_{sh} increasing from 103 Ω/cm^2 to 308 Ω/cm^2 after modified with ILCNs. The R_s of PSCs with 15 nm ZnO layer after modified with ILCNs almost has no change and its R_{sh} increasing from 279 Ω/cm^2 to 431 Ω/cm^2. This means that the inferior interface contact between ZnO and P3HT:PCBM due to severely rough ZnO layer surface can be greatly improved after modified with ILCNs. ILCNs have almost no effect to improve the interface barrier for PSCs with 15 nm ZnO layer and can still improve shunt resistance. In other words, a 15 nm thick ZnO layer deposited with magnetic sputtering technique has superior surface property, sufficing to ensure electrons of the active layer favorably transfer to ZnO layer.

Impedance spectroscopy is a powerful technique to derive insights into the interfacial properties and the charge carrier dynamics of PSCs [28]. The different interface barrier between ZnO layer and the active layer is expected to affect carrier accumulation and transportation, resulting in differences in the device capacitance. Fig. 4 shows the impedance spectra of PSCs with different thickness ZnO layer modified with/without ILCNs in the dark. The complex impedance plots of Fig. 4c exhibits an arc in the fourth quadrant at the low frequency range at the voltage from 0.4 V to 0.6 V, indicating the negative capacitance exists in PSCs with 60 nm ZnO layer. After modified with ILCNs, the –Im(Z) values are always positive at any voltages and frequencies, as shown in Fig. 4d. However, the negative capacitive behavior never appears at any voltages and frequencies for PSCs with 15 nm and 30 nm ZnO buffer layer, as illustrated in Fig. 4a and b. Garcia-Belmonte et al. reported that the negative capacitive behavior would be appeared due to the Schottky contact at P3HT:PCBM/Al [28]. The massive electrons were accumulated in the vicinity of cathode due to high interface barrier under moderate forward bias, which can result in the negative capacitive behavior. The negative capacitive behavior of P3HT:PCBM/Al

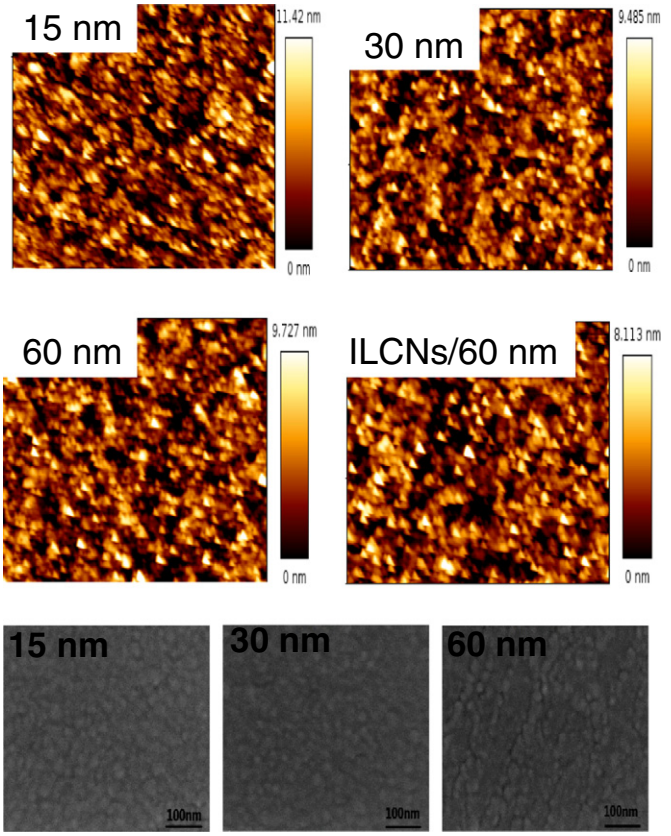

Fig. 3. Surface morphology AFM and SEM images of 15-nm, 30-nm, and 60-nm thick ZnO layers and AFM image of ILCNs modified 60 nm ZnO layer deposited on ITO substrate.

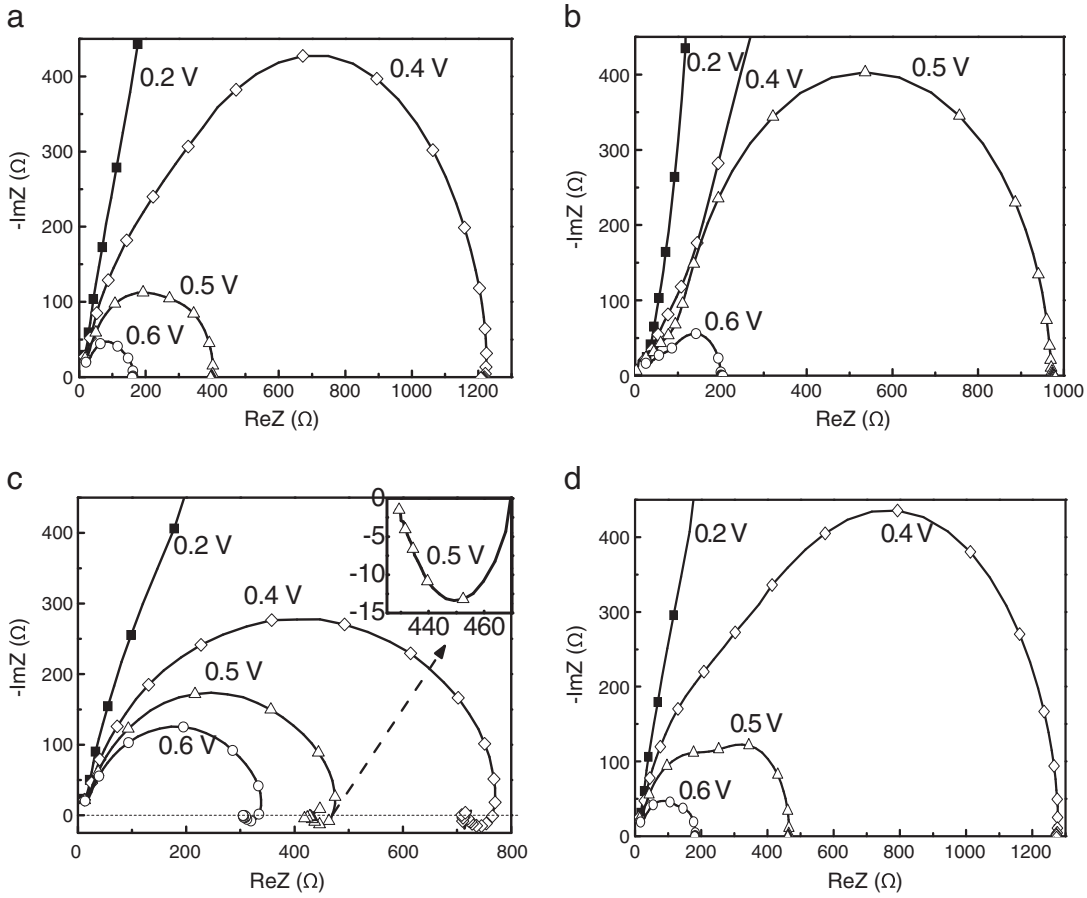

Fig. 4. Bias dependence of cole–cole plots of inverted PSCs with ZnO layer thickness 15 nm (a), 30 nm (b), 60 nm (c) and ILCNs modified 60 nm ZnO layer (d).

disappeared after ILCNs modified with Al cathode was further reported by Chen et al. [20], indicating low interface barrier or ohmic contacts at the cathode. Similarly, the negative capacitive behavior in PSCs with 60 nm ZnO layer may be attributed to the electron accumulation at the interface of ZnO/P3HT:PCBM due to high contact barrier. The obviously electron accumulation under moderate forward bias didn't appear for 15 nm and 30 nm thick ZnO layers, indicating low rough ZnO surface is helpful to decrease interface barrier at the interface of ZnO/P3HT:PCBM.

4. Conclusion

In summary, the surface property and thickness of ZnO layer as an electron selective layer significantly affects PCE of inverted P3HT:PCBM based PSCs. The average PCE of PSCs with ZnO layer thickness ranging from 15 nm to 30 nm is almost comparable to that of traditional PSCs with PEDOT:PSS anode buffer layer. Average PCE of PSCs was decreased to 2.65% for 60 nm ZnO layer and increased to 3.44% using ILCNs modified 60 nm ZnO layer, approaching that of PSCs with 15 nm and 30 nm ZnO layers. The severe surface roughness of 60 nm ZnO layer compared to 15 nm and 30 nm ZnO layers results in high interface contact barrier at the interface of ZnO/P3HT:PCBM. The PCE of inverted PSCs based on ZnO electron selective layer deposited with magnetron sputtering method is more sensitive to the surface roughness of ZnO films than ZnO layer thickness. The efficient inverted PSCs based on P3HT:PCBM blend achieved with wide range of ZnO layer thickness indicates that magnetron sputtering deposition is an easily controlling method to fabricate ZnO layer as a good electron selective layer. This strategy can be expected to apply to highest efficiency polymer devices since solution-processable ZnO layer has been still demonstrated a favorable electron selective layer for high efficiency polymer material [3,4].

Acknowledgment

This work was supported by National Natural Science Foundation of China (grant Nos. 61275038, 11274119), Natural Science Foundation of Shanghai Science and Technology Commission (grant No. 11ZR1411300), Pujiang Talent Program of Shanghai Science and Technology Commission (grant No.11PJ1402700), Doctoral Fund of Ministry of Education of China (grant No.20110076120017) and SRF for ROCS, SEM.

References

[1] M.T. Lloyd, C.H. Peters, A. Garcia, I.V. Kauvar, J.J. Berry, M.O. Reese, M.D. McGehee, D.S. Ginley, D.C. Olson, Sol. Energy Mater. Sol. Cells 95 (2011) 1382.
[2] C.J. Brabec, S. Gowrisanker, J.J.M. Halls, D. Laird, S. Jia, S.P. Williams, Adv. Mater. 22 (2010) 3839.
[3] J. You, L. Dou, K. Yoshimura, T. Kato, K. Ohya, T. Moriarty, K. Emery, C.-C. Chen, J. Gao, G. Li, Nat. Commun. 4 (2013) 1446.
[4] Z. He, C. Zhong, S. Su, M. Xu, H. Wu, Y. Cao, Nat. Photonics 6 (2012) 593.
[5] M. Jørgensen, K. Norrman, F.C. Krebs, Sol. Energy Mater. Sol. Cells 92 (2008) 686.
[6] L.M. Chen, Z. Hong, G. Li, Y. Yang, Adv. Mater. 21 (2009) 1434.
[7] M.D. Irwin, D.B. Buchholz, A.W. Hains, R.P.H. Chang, T.J. Marks, Proc. Natl. Acad. Sci. 105 (2008) 2783.
[8] A. Kyaw, X. Sun, C. Jiang, G. Lo, D. Zhao, D. Kwong, Appl. Phys. Lett. 93 (2008) 221107.
[9] S.K. Hau, H.-L. Yip, N.S. Baek, J. Zou, K. O'Malley, A.K.-Y. Jen, Appl. Phys. Lett. 92 (2008) 253301.
[10] J.C. Wang, W.T. Weng, M.Y. Tsai, M.K. Lee, S.F. Horng, T.P. Perng, C.C. Kei, C.C. Yu, H.F. Meng, J. Mater. Chem. 20 (2010) 862.
[11] Y.-S. Park, K.-H. Choi, H.-K. Kim, J. Phys. D. Appl. Phys. 42 (2009) 235109.
[12] Y. Jouane, S. Colis, G. Schmerber, P. Kern, A. Dinia, T. Heiser, Y.A. Chapuis, J. Mater. Chem. 21 (2010) 1953.
[13] J. Hu, Z. Wu, H. Wei, T. Song, B. Sun, Org. Electron. 13 (2012) 1171.
[14] J.A. Jeong, H.K. Kim, Sol. Energy Mater. Sol. Cells 93 (2009) 1801.

[15] C. Guillén, J. Herrero, Thin Solid Films 520 (2011) 1.
[16] K.H. Kim, K.C. Park, D.Y. Ma, J. Appl. Phys. 81 (1997) 7764.
[17] J.A. Jeong, H.K. Kim, M.S. Yi, Appl. Phys. Lett. 93 (2008) 033301.
[18] W. Potscavage, S. Yoo, B. Domercq, B. Kippelen, Appl. Phys. Lett. 90 (2007) 253511.
[19] H.K. Kim, M.S. Kim, J.W. Kang, J.J. Kim, M.S. Yi, Appl. Phys. Lett. 90 (2007) 013502.
[20] X. Chen, J. Yang, J. Lu, K.K. Manga, K.P. Loh, F. Zhu, Appl. Phys. Lett. 95 (2009) 133305.
[21] J. Lu, J. Yang, J. Wang, A. Lim, S. Wang, K.P. Loh, ACS Nano 3 (2009) 2367.
[22] Z. Liang, Q. Zhang, O. Wiranwetchayan, J. Xi, Z. Yang, K. Park, C. Li, G. Cao, Adv. Funct. Mater. 22 (2012) 2194.
[23] X. Chen, J. Yang, L.Y.X.C. Haley, J. Lu, F. Zhu, K.P. Loh, Org. Electron. 11 (2010) 1942.
[24] A. Tada, Y. Geng, M. Nakamura, Q. Wei, K. Hashimoto, K. Tajima, Phys. Chem. Chem. Phys. 14 (2012) 3713.
[25] R. Green, A. Morfa, A. Ferguson, N. Kopidakis, G. Rumbles, S. Shaheen, Appl. Phys. Lett. 92 (2008) 033301.
[26] Z. Hu, J. Zhang, Y. Zhao, Appl. Phys. Lett. 100 (2012) 103303.
[27] Z. Hu, J. Zhang, Y. Liu, Y. Li, X. Zhang, Y. Zhao, Synth. Met. 161 (2011) 2174.
[28] G. Garcia-Belmonte, A. Munar, E.M. Barea, J. Bisquert, I. Ugarte, R. Pacios, Org. Electron. 9 (2008) 847.